Pleiotropic mutations can rapidly evolve to directly benefit self and cooperative partner despite unfavorable conditions

Samuel F. M. Hart[1], Chi-Chun Chen[1], Wenying Shou[1,2 #]

[1] Fred Hutchinson Cancer Research Center, Division of Basic Sciences, Seattle, US

[2] University College London, Department of Genetics, Evolution and Environment, London, UK

(#: Author of correspondence, wenying.shou@gmail.com)

Abstract

Cooperation, paying a cost to benefit others, is widespread. Cooperation can be promoted by pleiotropic "win-win" mutations which directly benefit self ("self-serving") and partner ("partner-serving"). Previously, we showed that partner-serving should be defined as increased benefit supply rate per intake benefit (Hart & Pineda et al., 2019). Here, we report that win-win mutations can rapidly evolve even under conditions unfavorable for cooperation. Specifically, in a well-mixed environment we evolved engineered yeast cooperative communities where two strains exchanged costly metabolites lysine and hypoxanthine. Among cells that consumed lysine and released hypoxanthine, *ecm21* mutations repeatedly arose. *ecm21* is self-serving, improving self's growth rate in limiting lysine. *ecm21* is also partner-serving, increasing hypoxanthine release rate per lysine consumption and the steady state growth rate of partner. *ecm21* also arose in monocultures evolving in lysine-limited chemostats. Thus, even without any history of cooperation or pressure to maintain cooperation, pleiotropic win-win mutations may readily evolve.

Introduction

Cooperation, paying a fitness cost to generate benefits available to others – is widespread and thought to drive major evolutionary transitions [1,2]. For example in multi-cellular organisms, different cells must cooperate with each other and refrain from dividing in a cancerous fashion to

ensure the propagation of the germline [3]. Cooperation between species, or mutualistic cooperation, are also common [4]. In extreme cases, mutualistic cooperation are obligatory, *i.e.* cooperating partners depend on each other for survival [5,6]. For example, insects and endosymbiotic bacteria exchange costly essential metabolites [6,7].

Cooperation is vulnerable to "cheaters" who gain a fitness advantage over cooperators by consuming benefits without reciprocating fairly. Cancers are cheaters of multi-cellular organisms [8], and rhizobia variants can cheat on their legume hosts [9]. How might cooperation survive cheaters?

Various mechanisms are known to protect cooperation against cheaters. In “partner choice”, an individual preferentially interacts with cooperating partners over spatially-equivalent cheating partners [2,10–12]. For example, client fish observes cleaner fish cleaning other clients, and then chooses the cleaner fish that offers high-quality service (removing client parasites instead of client tissue) to interact with [11].

For organisms lacking partner choice mechanisms, a spatially-structured environment can promote the origin and maintenance of cooperation [2,13–18]. This is because in a spatially-structured environment neighbors repeatedly interact, and thus cheaters will eventually suffer as their neighbors perish (“partner fidelity feedback”). In a well-mixed environment, since all individuals share equal access to the cooperative benefit regardless of their contributions, cheaters are favored over cooperators [15]. An exception is that cooperators can stochastically purge cheaters if cooperators happen to be better adapted to an environmental stress than cheaters [19–21]. Finally, pleiotropy — a single mutation affecting multiple phenotypes — can stabilize cooperation if reducing benefit supply to partner also elicits a crippling effect on self [22–26]. For example, when the social amoeba *Dictyostelium discoideum* experience starvation and form a fruiting body, a fraction of the cells differentiate into a non-viable stalk in order to support the remaining cells to differentiation into viable spores. *dimA* mutants attempt to cheat by avoiding the stalk fate, but they also fail to form spores [22]. In this case, a gene links an individual’s partner-serving trait to its self-serving trait, thus stabilizing cooperation.

To date, pleiotropic linkage between a self-serving trait and a partner-serving trait has been exclusively demonstrated in systems with long evolutionary histories of cooperation. Thus, it is

unclear how easily such a genetic linkage can arise. One possibility is that cooperation promotes pleiotropy. Indeed, theoretical work suggests that cooperation can stabilize pleiotropy [27], and that pleiotropic linkage between self-serving and partner-serving traits is favored as cooperators evolve to resist cheater invasion [28]. A second possibility is that pleiotropy promotes cooperation [22–26]. These two possibilities are not mutually exclusive.

Here, we investigate whether pleiotropy existing before the onset of cooperation can stabilize nascent cooperation. Specifically, we test whether pleiotropic "win-win" mutations directly benefiting self and directly benefiting partner could arise in a synthetic cooperative community growing in an environment unfavorable for cooperation. The community is termed CoSMO (Cooperation that is Synthetic and Mutually Obligatory). CoSMO comprises two non-mating engineered *Saccharomyces cerevisiae* strains: $L^{-}H^{+}$ requires lysine (*L*) and pays a fitness cost to overproduce hypoxanthine (*H*, an adenine derivative) [21,29], while $H^{-}L^{+}$ requires hypoxanthine and pays a fitness cost to overproduce lysine [30] (Figure 1A). Overproduced metabolites are released into the environment by live cells [29], allowing the two strains to feed each other. CoSMO models the metabolic cooperation between certain gut microbial species [31] and between legumes and rhizobia [32], as well as other mutualisms [33–38]. Similar to natural systems, in CoSMO exchanged metabolites are costly to produce [21,29], and cooperation can transition to competition when the exchanged metabolites are externally supplied [39]. Importantly, principles learned from CoSMO have been found to operate in communities of un-engineered microbes. These include how fitness effects of interactions might affect spatial patterning and species composition in two-species communities [39], as well as how cooperators might survive cheaters [14,21] (see Discussions in these articles).

In our previous work, we allowed nine independent lines of CoSMO to evolve for over 100 generations in a well-mixed environment by performing periodic dilutions [29,40]. Throughout evolution, the two cooperating strains coexisted due to their metabolic co-dependence [39,40]. In a well-mixed environment, since partner-supplied benefits are uniformly distributed and equally available to all individuals, a self-serving mutation will be favored regardless of how it affects the partner. Indeed, all characterized mutants isolated from CoSMO displayed self-serving phenotypic changes [21,29,30], outcompeting their ancestor in community-like environments. Here, we report the identification of a pleiotropic win-win mutation which is both self-serving and

partner-serving. This win-win mutation also arose in the absence of the cooperative partner. Thus, cooperation-promoting win-win mutations can arise in a community without any evolutionary history of cooperation and in environments unfavorable to cooperation. Our work suggests the possibility of pre-existing pleiotropy stabilizing nascent cooperation in natural communities.

Results

Criteria of a win-win mutation

A win-win mutation is defined as a single mutation (e.g. a point mutation; a translocation; a chromosome duplication) that directly promotes the fitness of self ("self-serving") and the fitness of partner ("partner-serving"). To define "direct" here, we adapt the framework from Chapter 10 of [41]: A mutation in genotype *A* exerts a direct fitness effect on genotype *B* if the mutation can alter the growth rate of *B* even if the biomass of *A* is fixed [30].

For L^-H^+, a self-serving mutation should improve the growth rate of self by, for example, increasing cell's affinity for lysine (Figure 1B, orange). A self-serving mutation allows the mutant to outcompete a non-mutant. A partner-serving mutation should improve the growth rate of partner at a fixed self biomass. Since the partner requires hypoxanthine, a partner-serving mutation in L^-H^+ should increase the hypoxanthine supply rate per L^-H^+ biomass. Since the biomass of L^-H^+ is linked to lysine consumption, the partner-serving phenotype of L^-H^+ translates to hypoxanthine supply rate per lysine consumption, or equivalently, hypoxanthine release rate per cell (r_H) normalized by the amount of lysine consumed to make a cell (c_L) [30]. We call this ratio r_H/c_L "*H-L* exchange ratio" (Figure 1B, purple), which can be interpreted as the yield coefficient while converting lysine consumption to hypoxanthine release. Note that a partner-serving mutation will eventually feedback to promote self growth. Indeed, after an initial lag, the growth rate of partner, of self, and of the entire community reach the same steady state growth rate $\sqrt{\frac{r_H}{c_L}\frac{r_L}{c_H}}$, where r_L (lysine release rate per cell) and c_H (hypoxanthine consumption amount per cell) are phenotypes of H^-L^+ [30].

Community and monoculture evolution share similar mutations

We randomly isolated evolved L^-H^+ colonies from CoSMO, and subjected them to whole-genome sequencing. Nearly every sequenced clone harbored one or more of the following mutations: *ecm21*, *rsp5*, and duplication of chromosome 14 (*DISOMY14*) (Table 1, top), consistent with our earlier studies [21,29,30,42]. Mutations in *RSP5*, an essential gene, mostly involved point mutations (e.g. *rsp5*(*P772L*)), while mutations in *ECM21* mostly involved premature stop codons and frameshift mutations (Table 1, top; Figure 2 Figure Supplement 1). Similar mutations also repeatedly arose when L^-H^+ evolved as a monoculture in lysine-limited chemostats (Table 1, bottom), suggesting that these mutations emerged independently of the partner.

Self-serving mutations increase the abundance of metabolite permease on cell surface

Evolved L^-H^+ clones are known to display a self-serving phenotype: they could form microcolonies on low-lysine plates where the ancestor failed to grow [21,30]. To quantify this self-serving phenotype, we used a fluorescence microscopy assay [43] to measure the growth rates of ancestral and evolved L^-H^+ in various concentrations of lysine. Under lysine limitation characteristic of the CoSMO environment (Figure 2A, "Comm. environ."), evolved L^-H^+ clones containing an *ecm21* or *rsp5* mutation grew faster than a *DISOMY14* strain which, as we showed previously, grew faster than the ancestor [30]. An engineered *ecm21Δ* or *rsp5*(*P772L*) mutation was sufficient to confer the self-serving phenotype (Figure 2A). In competition experiments in lysine-limited chemostats (8-hr doubling time), *ecm21Δ* rapidly outcompeted ancestral cells since *ecm21Δ* grew 4.4 times as fast as the ancestor (Figure 2- Figure Supplement 2).

A parsimonious explanation for *ecm21*'s self-serving phenotype is that during lysine limitation, the high-affinity lysine permease Lyp1 is stabilized on cell surface in the mutant. We have previously shown that duplication of the *LYP1* gene, which resides on Chromosome 14, is necessary and sufficient for the self-serving phenotype of *DISOMY14* [30]. Rsp5, an E3 ubiquitin ligase, is recruited by various "adaptor" proteins to ubiquitinate and target membrane transporters including Lyp1 for endocytosis and vacuolar degradation [44]. In high lysine, Lyp1-GFP was localized to both cell membrane and vacuole in ancestral and *ecm21* cells, but localized

to the cell membrane in *rsp5* cells (Figure 2B, top row). Thus, Lyp1 localization was normal in *ecm21* but not in *rsp5*, consistent with the notion that at high lysine concentrations, Lyp1 is targeted for ubiquitination by Rsp5 through the Art1 instead of the Ecm21 adaptor [44]. When ancestral $L^{-}H^{+}$ was incubated in low lysine, Lyp1-GFP was initially localized on the cell membrane to facilitate lysine uptake, but later targeted to the vacuole for degradation and recycling [45] (Figure 2B middle and bottom panels). However, in both *ecm21Δ* and *rsp5*(*P772L*) mutants, Lyp1-GFP was stabilized on cell membrane during prolonged lysine limitation (Figure 2B bottom panels). This could allow mutants to grow faster than the ancestor during lysine limitation.

ecm21 mutation is partner-serving

The partner-serving phenotype of $L^{-}H^{+}$ (i.e. hypoxanthine release rate per lysine consumption; exchange ratio r_H/c_L) can be measured in lysine-limited chemostats. In chemostats, fresh medium containing lysine was supplied at a fixed slow flow rate (mimicking the slow lysine supply by partner), and culture overflow exited the culture vessel at the same flow rate. After an initial lag, live and dead population densities reached a steady state (Figure 3- Figure supplement 1) and therefore, the net growth rate must be equal to the chemostat dilution rate *dil* (flow rate/culture volume). The released hypoxanthine also reached a steady state (Figure 3A). The *H-L* exchange ratio can be quantified as $dil * H_{ss}/L_0$ [30], where *dil* is the chemostat dilution rate, H_{ss} is the steady state hypoxantine concentration in the culture vessel, and L_0 is the lysine concentration in the inflow medium (which was fixed across all experiments). Note that this measure at the population level ($dil * H_{ss}/L_0$) is mathematically identical to an alternative measure at the individual level (hypoxanthine release rate per cell/lysine consumption amount per cell or r_H/c_L) [30].

Compared to the ancestor, *ecm21*Δ but not *DISOMY14* [30] or *rsp5*(*P772L*) exhibited increased *H-L* exchange ratio. Specifically, at the same dilution rate (corresponding to 6-hr doubling), the steady state hypoxanthine concentration was the highest in *ecm21*Δ, and lower in the ancestor, *DISOMY14* [30], and *rsp5*(*P772L*) (Figure 3A). Although exchange ratio depends on growth rate (*dil*), exchange ratios of *ecm21*Δ consistently outperformed those of the ancestor across doubling times typically found in CoSMO (Figure 3B). Thus, compared to the ancestor, *ecm21*Δ has a

higher hypoxanthine release rate per lysine consumption. This can be interpreted as improved metabolic efficiency in the sense of turning a fixed amount of lysine into a higher hypoxanthine release rate.

To test whether *ecm21*Δ can promote partner growth rate, we quantified the steady state growth rate of the H^-L^+ partner when cocultured with either ancestor or *ecm21*Δ L^-H^+ in CoSMO communities. After an initial lag, CoSMO reached a steady state growth rate [46] (constant slopes in Figure 4A). The same steady state growth rate was also achieved by the two cooperating strains [46]. Compared to the ancestor, *ecm21*Δ indeed sped up the steady state growth rate of CoSMO and of partner H^-L^+ (Figure 4B). Thus, *ecm21*Δ is partner-serving.

The partner-serving phenotype of *ecm21*Δ can be explained by the increased hypoxanthine release rate per lysine consumption, rather than the evolution of any new metabolic interactions. Specifically, the growth rate of partner H^-L^+ (and of community) is approximately the geometric mean of the two strains' exchange ratios, or $\sqrt{\frac{r_H}{c_L}\frac{r_L}{c_H}}$ [29,46]. Here, the ancestral partner's exchange ratio ($\frac{r_L}{c_H}$) is fixed, while the exchange ratio of L^-H^+ ($\frac{r_H}{c_L}$) is ~1.6-fold increased in *ecm21*Δ compared to the ancestor (at doubling times of 6~8 hrs; Figure 3B). Thus, *ecm21*Δ is predicted to increase partner growth rate by $\sqrt{1.6}-1$ =26% (95% confidence interval: 12%~38%; Figure 3 Source Data). In experiments, *ecm21*Δ increased partner growth rate by ~21% (Figure 4B; Figure 4 Source Data).

In conclusion, when L^-H^+ evolved in nascent mutualistic communities and in chemostat monocultures in a well-mixed environment, win-win *ecm21* mutations repeatedly arose (Table 1). Thus, pleiotropic win-win mutations can emerge in the absence of any prior history of cooperation, and in environments unfavorable for cooperation.

Discussions

The evolution of win-win mutations

Here, we have demonstrated that pleiotropic win-win mutations can rapidly arise. As expected, all evolved L^-H^+ clones displayed self-serving phenotypes, achieving a higher growth rate than the ancestor in low lysine presumably by stabilizing the lysine permease Lyp1 on cell membrane

(Figure 2) [30]. Surprisingly, *ecm21* mutants also displayed partner-serving phenotypes, promoting the steady state growth rate of partner H^-L^+ and of community (Figure 4) via increasing the hypoxanthine release rate per lysine consumption (Figure 3).

The partner-serving phenotype of L^-H^+ emerged as a side-effect of adaptation to lysine limitation instead of adaptation to a cooperative partner. We reached this conclusion because *ecm21* mutations were also observed in L^-H^+ evolving as monocultures in lysine-limited chemostats (Table 1). Being self-serving does not automatically lead to a partner-serving phenotype. For example in the *DISOMY14* mutant, duplication of the lysine permease *LYP1* improved mutant's affinity for lysine (Figure 2) without improving hypoxanthine release rate per lysine consumption (Figure 3A) or partner's growth rate [30].

How might *ecm21* mutants achieve higher hypoxanthine release rate per lysine consumption? One possibility is that purine overproduction is increased in *ecm21* mutants, leading to a steeper concentration gradient across the cell membrane. A different, and not mutually exclusive, possibility is that in *ecm21* mutants, purine permeases are stabilized much like the lysine permease, which in turn leads to increased membrane permeability. Future work will reveal the molecular mechanisms of this increased exchange ratio.

The win-win effect of *ecm21* is with respect to the ancestor. *ecm21* may disappear from a population due to competition with fitter mutants. If *ecm21* is fixed in L^-H^+, then a new state of faster community growth (Fig 4B) will be established. An interesting future direction would be to investigate whether during long-term evolution of CoSMO, other win-win mutations can occur in the *ecm21* background or in backgrounds that can outcompete *ecm21*, or in the partner strain.

How might nascent cooperation be stabilized?

A spatially-structured environment is known to facilitate the origin and maintenance of cooperation [2,13–18]. Here, we discuss three additional mechanisms that can stabilize nascent cooperation, even when the environment is well-mixed.

First, nascent cooperation can sometimes be stabilized by physiological responses to a new environment. For example, the mutualism between two metabolically-complementary *E. coli* strains was enhanced when one strain over-released metabolites after encountering the partner [51].

Interestingly, L^-H^+ cells increased its hypoxanthine release rate in the presence of low lysine (which mimics the presence of cooperative partners) compared to in the absence of lysine (which mimics the absence of cooperative partners, although without lysine consumption, an exchange ratio cannot be calculated) [29].

Second, nascent cooperation can be stabilized by self-benefiting changes that, through promoting self-fitness, *indirectly* promote partner's fitness. Consider a mutant with improved affinity for lysine but no alterations in the metabolite exchange ratio (e.g. *DISOMY14* [30]). By growing better in low lysine, this mutant will improve its own survival which in turn helps the whole community (and thus the partner) to survive the initial stage of low cell density. Indeed, all evolved L^-H^+ clones tested so far improved community (and partner) survival in the sense that all mutants reduced the minimal total cell density required for the community to grow to saturation [21,40]. Unlike *ecm21*, some of these mutations (e.g. *DISOMY14*) are not directly partner-serving, and would not improve partner's steady state growth rate [30].

Third, nascent cooperation can be stabilized by pleiotropic win-win mutations which *directly* promote self-fitness (by increasing competitiveness against non-mutants) and *directly* promote partner fitness (by increasing benefit supply rate per intake benefit). In this study, win-win mutations in *ecm21* rapidly evolved in a well-mixed environment, even in the absence of cooperative partner or any evolutionary history of cooperation.

Pleiotropy and cooperation

Pleiotropic linkage between a self-serving trait and a partner-serving trait arises when both traits are controlled by the same gene (co-regulated) [27]. For example, the quorum sensing network of *Pseudomonas aeruginosa* ties together a cell's ability to make "public goods" (such as extracellular proteases that provide a benefit to the local population) with the cell's ability to make "private goods" (such as intracellular enzymes involved in metabolism) [23]. Consequently, *LasR* mutants that "cheat" by not secreting protease also fail to metabolize adenosine for themselves [23].

Pleiotropy might be common, given that gene networks display "small world" connectivity [52] and that a protein generally interacts with many other proteins. Indeed, pleiotropic linkage between self-serving and partner-serving traits has been observed in several natural cooperative

systems [22–26], and is thought to be important for cooperation [22–26,28,47–49]. However, such linkage can be broken during evolution [27,50]. In our evolution experiments, win-win *ecm21* mutations repeatedly rose to be readily detectable in independent lines (Table 1), and promoted both community growth rate (Figure 4) and community survival at low cell densities [21]. Future work will reveal the evolutionary persistence of win-win mutations and their phenotypes.

In known examples of pleiotropic linkages between self-serving and partner-serving traits, cooperation has a long evolutionary history, and is intra-population. Our work demonstrates that pleiotropy can give rise to win-win mutations that promote nascent, mutualistic cooperation. Interestingly, win-win mutation(s) have also been identified in a different engineered yeast cooperative community where two strains exchange leucine and tryptophane [53] (Andrew Murray, personal communications). As another example, in a synthetic mutualistic community between un-engineered *E. coli* and un-engineered N_2-fixing *Rhodopseudomonas palustris*, a mutation in *E. coli* that improves the uptake of partner-supplied nutrients improved community growth rate (and final yield), suggesting that this mutation may also be win-win [54]. Overall, these observations in synthetic communities raise the possibility that pre-existing pleiotropy may have stabilized nascent cooperation in natural communities. Future work, including unbiased screens of many mutations in synthetic cooperative communities of diverse organisms, will reveal how pleiotropy might impact nascent cooperation.

Methods

Strains

Our nomenclature of yeast genes, proteins, and mutations follows literature convention. For example, the wild type *ECM21* gene encodes the Ecm21 protein; *ecm21* represents a reduction-of-function or loss-of-function mutation. Our *S. cerevisiae* strains are of the RM11-1a background. Both L^-H^+ (WY1335) and H^-L^+ (WY1340) are of the same mating type (*MATa*) and harbor the *ste3Δ* mutation to prevent mating between the two strains (Table S1). All evolved or engineered strains used in this paper are summarized in Table 1 and Supplementary File 1.

Growth medium and strain culturing have been previously discussed [30].

Experimental evolution

CoSMO evolution has been described in detail in [30]. Briefly, exponentially-growing L^-H^+ (WY1335) and H^-L^+ (WY1340) were washed free of supplements, counted using a Coulter counter, and mixed at 1000:1 (Line A), 1:1 (Line B), or 1:1000 (Line C) at a total density of $5x10^5$/ml. Three 3ml community replicates (replicates 1, 2, and 3) per initial ratio were initiated, thus constituting nine independent lines. Since the evolutionary outcomes of the nine lines were similar, they could be treated as a single group. Communities were grown at 30°C in glass tubes on a rotator to ensure well-mixing. Community turbidity was tracked by measuring the optical density (OD_{600}) in a spectrophotometer once to twice every day. In this study, 1 OD was found to be 2~4x10^7cells/ml. We diluted communities periodically to maintain OD at below 0.5 to avoid additional selections due to limitations of nutrients other than adenine or lysine. The fold-dilution was controlled to within 10~20 folds to minimize introducing severe population bottlenecks. Coculture generation was calculated from accumulative population density by multiplying OD with total fold-dilutions. Sample were periodically frozen down at -80°C. To isolate clones, a sample of frozen community was plated on rich medium YPD and clones from the two strains were distinguished by their fluorescence colors or drug resistance markers.

For chemostat evolution of L^-H^+, device fabrication and setup are described in detail in [42]. Briefly, the device allowed the evolution of six independent cultures, each at an independent doubling time. To inoculate each chemostat vessel, ancestral L^-H^+ (WY1335) was grown to

exponential phase in SD supplemented with 164 μM lysine. The cultures were washed with SD and diluted to OD600 of 0.1 (~$7x10^6$/ml) in SD. 20 ml of diluted culture was added to each vessel through the sampling needle, followed by 5 ml SD to rinse the needle of excess cells. Of six total chemostat vessels, each containing ~43mL running volume, three were set to operate at a target doubling time of 7 hours (flow rate ~4.25 mL/hr), and three were set to an 11 hour target doubling time (flow rate ~2.72 mL/hr). With 21 μM lysine in the reservoir, the target steady state cell density was $7x10^6$/ml. In reality, live cell densities varied between $4x10^6$/ml and $1.2x10^7$/ml. Samples were periodically taken through a sterile syringe needle. The nutrient reservoir was refilled when necessary by injecting media through a sterile 0.2 micron filter through a 60-ml syringe. We did not use any sterile filtered air, and were able to run the experiment without contamination for 500 hours. Some reservoirs (and thus vessels) became contaminated after 500 hours.

Whole-genome sequencing of evolved clones and data analysis were described in detail in [30].

Quantification methods

Microscopy quantification of L^-H^+ growth rates at various lysine concentrations was described in [29,43]. Briefly, cells were diluted into flat-bottom microtiter plates to low densities to minimize metabolite depletion during measurements. Microtiter plates were imaged periodically (every 0.5~2 hrs) under a 10x objective in a temperature-controlled Nikon Eclipse TE-2000U inverted fluorescence microscope. Time-lapse images were analyzed using an ImageJ plugin Bioact [43]. We normalized total fluorescence intensity against that at time zero, calculated the slope of ln(normalized total fluorescence intensity) over three to four consecutive time points, and chose the maximal value as the growth rate corresponding to the input lysine concentration. For validation of this method, see [43].

Short-term chemostat culturing of L^-H^+ for measuring exchange ratio was described in [29,43]. Briefly, because L^-H^+ rapidly evolved in lysine-limited chemostat, we took special care to ensure the rapid attainment of steady state so that an experiment is kept within 24 hrs. We set the pump flow rate to achieve the desired doubling time T (19ml culture volume*ln(2)/T). Periodically, we sampled chemostats to measure live and dead cell densities, and the concentration of released hypoxanthine.

Cell density measurement via flow cytometry was described in [29]. Briefly, we mixed into each sample a fixed volume of fluorescent bead stock whose density was determined using a hemocytometer or Coulter counter. From the ratio between fluorescent cells or non-fluorescent cells to beads, we can calculate live cell density and dead cell density, respectively.

Chemical concentration measurement was performed via a yield-based bioassay [29]. Briefly, the hypoxanthine concentration in an unknown sample was inferred from a standard curve where the final turbidities of an *ade-* tester strain increased linearly with increasing concentrations of input hypoxanthine.

Quantification of CoSMO growth rate was described in [29]. Briefly, we used the "spot" setting where a 15 µl drop of CoSMO community (1:1 strain ratio; ~$4x10^4$ total cells/patch) was placed in a 4-mm inoculum radius in the center of a 1/6 Petri-dish agarose sector. During periodic sampling, we cut out the agarose patch containing cells, submerged it in water, vortexed for a few seconds, and discarded agarose. We then subjected the cell suspension to flow cytometry.

Imaging of GFP localization

Cells were grown to exponential phase in SD plus 164µM lysine. A sample was washed with and resuspended in SD. Cells were diluted into wells of a Nunc 96-well Optical Bottom Plate (Fisher Scientific, 165305) containing 300µl SD supplemented with 164µM or 1µM lysine. Images were acquired under a 40X oil immersion objective in a Nikon Eclipse TE2000-U inverted fluorescence microscope equipped with a temperature-controlled chamber set at 300C. GFP was imaged using an ET-EYFP filter cube (Exciter: ET500/20x, Emitter: ET535/30m, Dichroic: T515LP). Identical exposure times (500 msec) were used for both evolved and ancestral cells.

Introducing mutations into the essential gene RSP5

Since *RSP5* is an essential gene, the method of deleting the gene with a drug-resistance marker and then replacing the marker with a mutant gene cannot be applied. We therefore modified a two-step strategy [55] to introduce a point mutation found in an evolved clone into the ancestral L^-H^+ strain. First, a loxP-kanMX-loxP drug resistance cassette was introduced into ~300 bp after the stop codon of the mutant *rsp5* to avoid accidentally disrupting the remaining function in *rsp5*. Second, a region spanning from ~250 bp upstream of the point mutation [C(2315)→T] to immediately after the loxP-kanMX-loxP drug resistance

362 cassette was PCR-amplified. The PCR fragment was transformed into a wild-type strain lacking *kanMX*.
363 G418-resistant colonies were selected and PCR verified for correct integration (11 out of 11 correct). The
364 homologous region during transformation is large, and thus recombination can occur in such a way that
365 the transformant got the *KanMX* marker but not the mutation. We therefore Sanger-sequenced the region,
366 found that 1 out of 11 had the correct mutation, and proceeded with that strain.

367

Figures

Figure 1. Win-win mutation in a nascent cooperative community

Figure 1 (**A**) CoSMO consists of two non-mating cross-feeding yeast strains, each engineered to overproduce a metabolite required by the partner strain. Metabolite overproduction is due to a mutation that renders the first enzyme of the biosynthetic pathway resistant to end-product inhibition [56,57]. Hypoxanthine and lysine are released by live L^-H^+ and live H^-L^+ cells at a per cell rate of r_H and r_L, respectively [29], and are consumed by the partner at a per cell amount of c_H and c_L, respectively. The two strains can be distinguished by different fluorescent markers. (**B**) **Win-win mutation**. A pleiotropic win-win mutation confers a self-serving phenotype (orange) and a partner-serving phenotype (lavender).

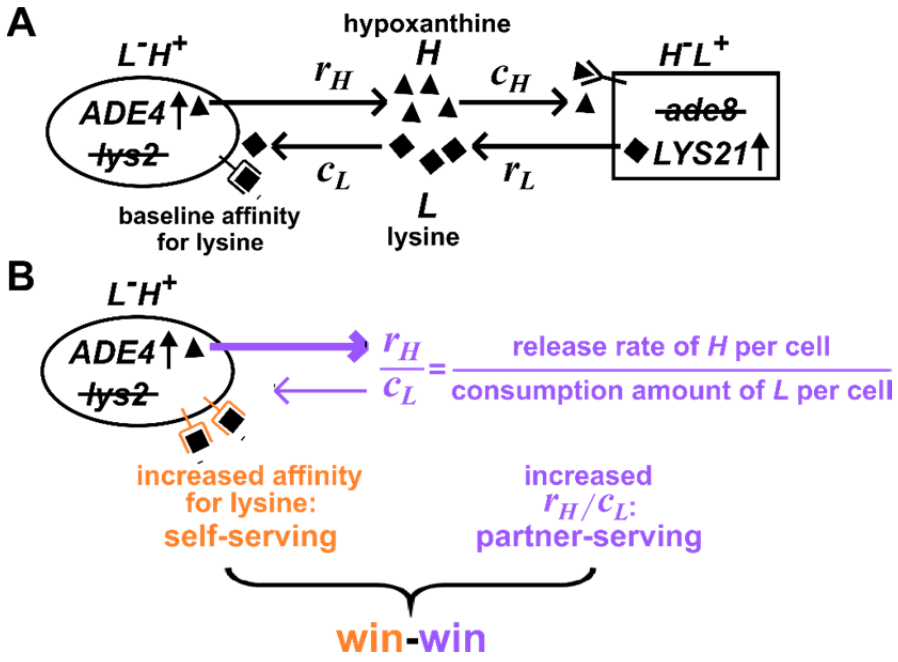

Figure 2. Self-serving mutations stabilize the high affinity lysine permease Lyp1 on cell membrane and improve cell growth rates at low lysine

Figure 2 **(A) Recurrent mutations are self-serving**. We measured growth rates of mutant and ancestral strains in minimal SD medium with various lysine concentrations, using a calibrated fluorescence microscopy assay [43]. Briefly, for each sample, total fluorescence intensity of image frames were tracked over time, and the maximal positive slope of ln(fluorescence intensity) against time was used as the growth rate. Evolved strains grew faster than the ancestor in community environment (the grey dotted line demarcating "Comm. environ." corresponds to the lysine level supporting a growth rate of 0.1/hr as observed in ancestral CoSMO [29]). Measurements performed on independent days (≥ 3 trials) were pooled and the average growth rate is plotted. Fit lines are based on Moser's equation for the birth rate b as a function of metabolite concentration L: $b(L)=b_{max}L^n/(K_L^n+L^n)$, where b_{max} is maximum birth rate in excess lysine, K_L is the lysine concentration at which half maximum birth rate is achieved, and n is the cooperitivity cooeficient describing the sigmoidal shape of the curve [58]. Evolved strains are marked with "*evo*"; engineered or backcrossed mutants are marked with the genotype. Data for *DISOMY14* are reproduced from [30] as a comparison. Data can be found in "Figure 2 Source Data". **(B) Self-serving mutations stabilize Lyp1 localization on cell membrane.** We fluorescently tagged Lyp1 with GFP in ancestor (WY1620), *ecm21Δ* (WY2355), and *rsp5*(*P772L*) (WY2356) to observe Lyp1 localization. We imaged each strain in a high lysine concentration (164 μM) as well as after 4 and 10 hours incubation in low lysine (1 μM). Note that low lysine was not consumed during incubation [43]. During prolonged lysine limitation, Lyp1 was stabilized to cell membrane in both mutants compared to the ancestor.

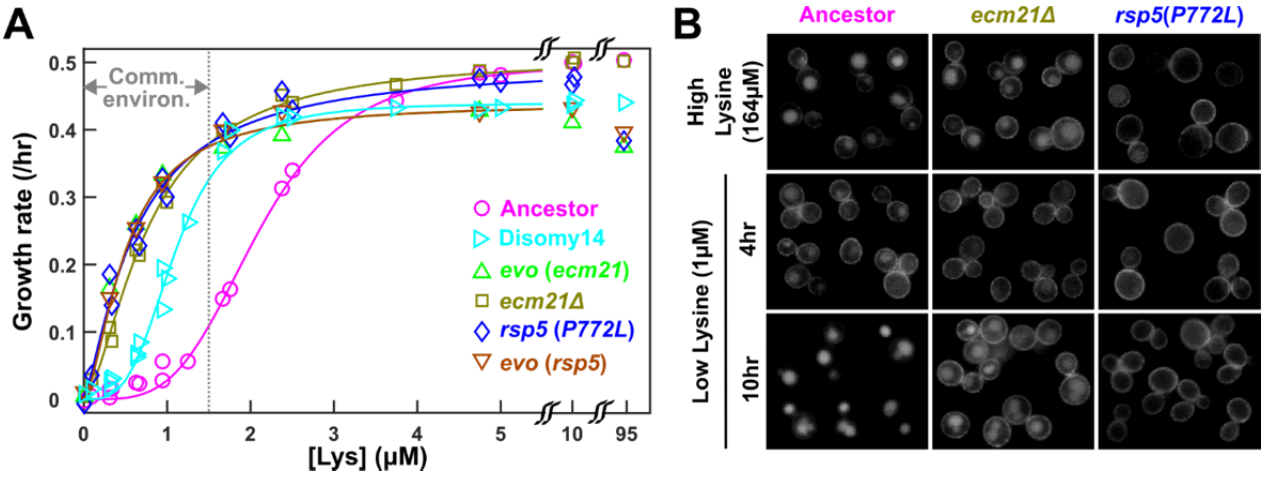
A
Comm. environ.
Growth rate (/hr)
0.5
0.4
0.3
0.2
0.1
0
0
1
2
3
4
5
10
95
[Lys] (μM)
Ancestor
Disomy14
evo (ecm21)
ecm21Δ
rsp5 (P772L)
evo (rsp5)
B
Ancestor
ecm21Δ
rsp5(P772L)
High Lysine (164μM)
Low Lysine (1μM)
4hr
10hr

402
403

Figure 3. ecm21Δ improves hypoxanthine release rate per lysine consumption.

Figure 3 **(A) Hypoxanthine accumulates to a higher level in *ecm21Δ* chemostats than in ancestor chemostats.** We cultured individual strains in lysine-limited chemostats (20 μM input lysine) at 6-hr doubling time (similar to CoSMO doubling time). Periodically, we quantified live and dead cell densities using flow cytometry (Figure 3 Figure Supplement 1), and hypoxanthine concentration in filtered supernatant using a yield-based bioassay [29]. The steady state hypoxanthine concentration created by the ancestor (WY1335) was lower than e*cm21Δ* (WY2226), and slightly higher than *rsp5*(*P772L*) (WY2475). *DISOMY14* (WY2349) was indistinguishable from the ancestor, similar to our previous report [30]. **(B) *ecm21Δ* has a higher hypoxanthine-lysine exchange ratio than the ancestor**. Cells were cultured in lysine-limited chemostats that spanned the range of CoSMO environments. In all tested doubling times, the exchange ratios of *ecm21Δ* were significantly higher than those of the ancestor. The exchange ratios of *rsp5*(*P772L*) were similar to or lower than those of the ancestor. Mean and two standard deviations from 4~5 experiments are plotted. *p*-values are from two-tailed t-test assuming either unequal variance (4-hr doubling) or equal variance (6-hr and 8-hr doublings; verified by F-test). Data and *p*-value calculations can be found in "Figure 3 Source Data".

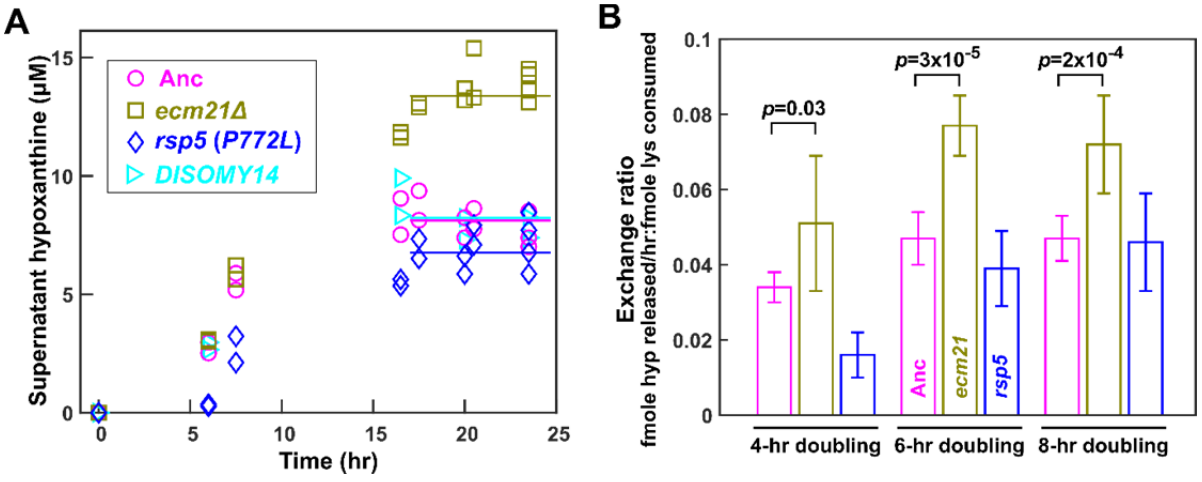

Figure 4. ecm21Δ increases the growth rate of CoSMO and of partner.

To prevent rapid evolution, we grew CoSMO containing ancestral H^-L^+ and ancestral or *ecm21Δ* L^-H^+ in a spatially-structured environment on agarose pads, and periodically measured the absolute abundance of the two strains using flow cytometry [29]. (**A**) **Growth dynamics**. After an initial lag, CoSMO achieved a steady state growth rate (slope of dotted line). (**B**) ***ecm21Δ* increases the growth rate of CoSMO and of partner.** Steady state growth rates of the entire community (left) and of partner H^-L^+ (right) were measured (n≥6), and the average and two standard deviations are plotted. *p*-values are from two-tailed t-test with equal variance (verified by F-test). The full data set and outcomes of statistical tests can be found in Figure 4 Source Data.

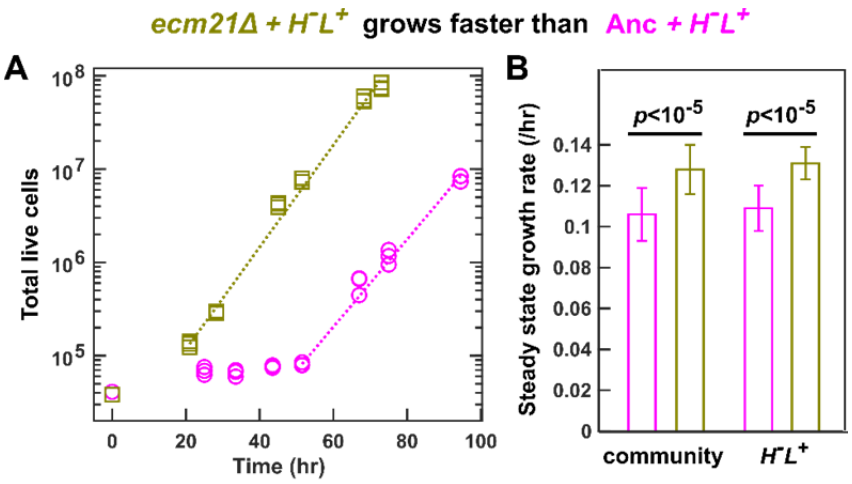

Figure 2-Figure Supplement 1. Functional domains and positions of mutations in Ecm21 and Rsp5 proteins

Mutations and their locations are marked with respect to the functional domains of the proteins. Numbers indicate amino acid positions, except in non-coding regions. Doman structures are obtained from the "protein" tab of SGD (https://www.yeastgenome.org/locus/S000000927/protein; https://www.yeastgenome.org/locus/S000000197/protein). HECT domain is found in ubiquitin-protein ligases. WW domain can bind proteins with particular proline-motifs such as the PPxY motif. Arrestin C-terminal-like domain is involved in signaling and endocytosis of receptors. For *ECM21*, mutating the three poly-proline-tyrosine (PY) motifs after amino acid 884 inhibited the stress-induced endocytosis of the manganese transporter Smf1 [59]. Most *ecm21* mutations we recovered introduced premature stop codons before the PY motifs. In *RSP5*, the region including and upstream of - 470 is required for *RSP5* function [60]. Mutations from coculture and monoculture isolates are marked above and below the gene, respectively.

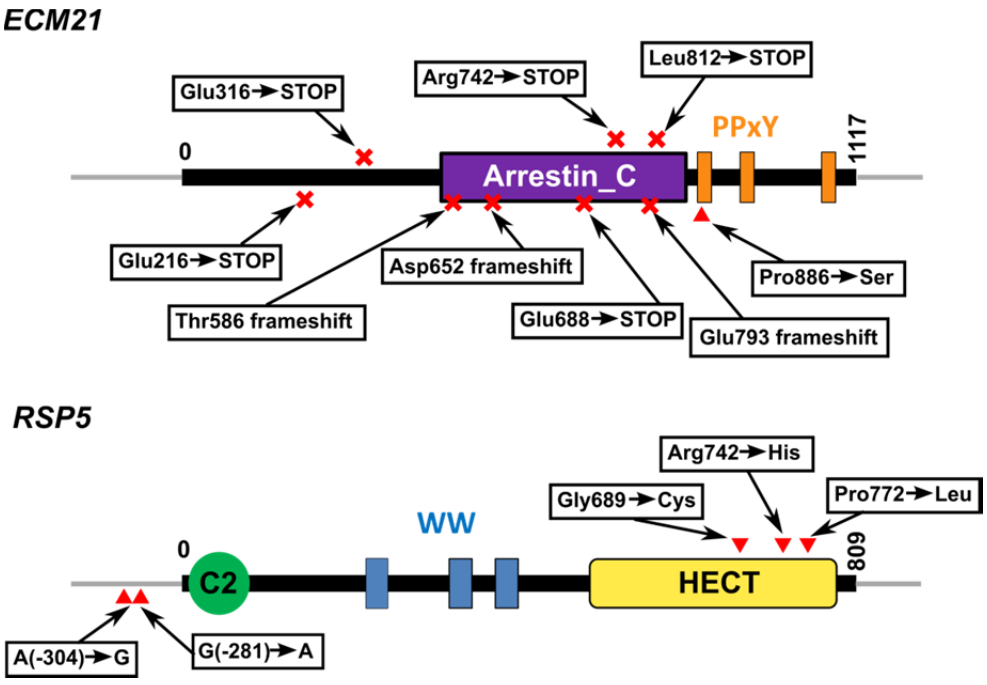

Figure 2 Figure Supplement 2 ecm21Δ rapidly outcompetes ancestor in lysine-limited chemostats.

We competed ancestor (expressing the mCherry fluorescent protein) and *ecm21Δ* (expressing the blue fluorescent protein) in four independent lysine-limited chemostats (represented by different symbols). Minimal medium containing 20 μM lysine is pumped in to achieve an 8-hr doubling time (similar to CoSMO doubling time). Periodically, we measured strain ratio using flow cytometry (Methods, "Quantification methods"). The fitness advantage of *ecm21Δ* over ancestor is 0.315±0.014 /hr (calculated from the slope using all data except the last time point when *ecm21Δ* had risen to be the majority). Since ancestor's growth rate is ln(2)/8=0.0866/hr, *ecm21Δ* grows 4.7 times as fast as the ancestor. This is consistent with Figure 2A: The ancestor achieves a doubling time of 8 hrs at 1.38 μM lysine, and at this concentration, *ecm21Δ* grows at 0.38/hr, 4.4 times as fast as the ancestor. Data can be found in "Figure 3 Figure Supplement 1 Source Data".

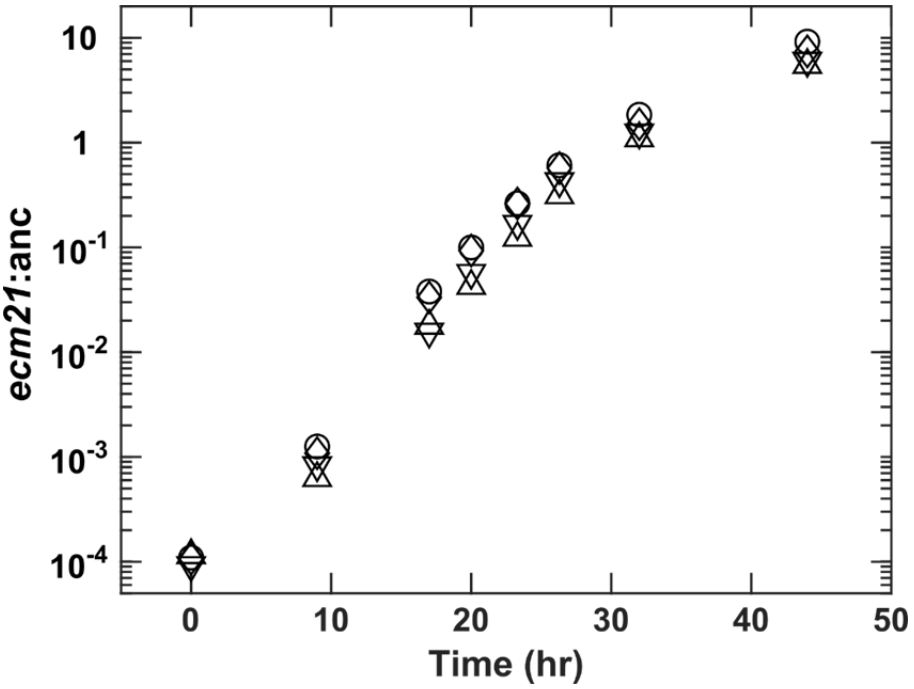

Figure 3 Figure Supplement 1 Population dynamics in chemostats.

We cultured ancestor and mutant strains in lysine-limited chemostats (20 μM input lysine) at 6-hr doubling time (similar to CoSMO doubling time). Periodically, we measured live and dead cell densities using flow cytometry [29]. After a lag, live and dead cell densities reached a steady state. Data can be found in "Figure 3 Source Data".

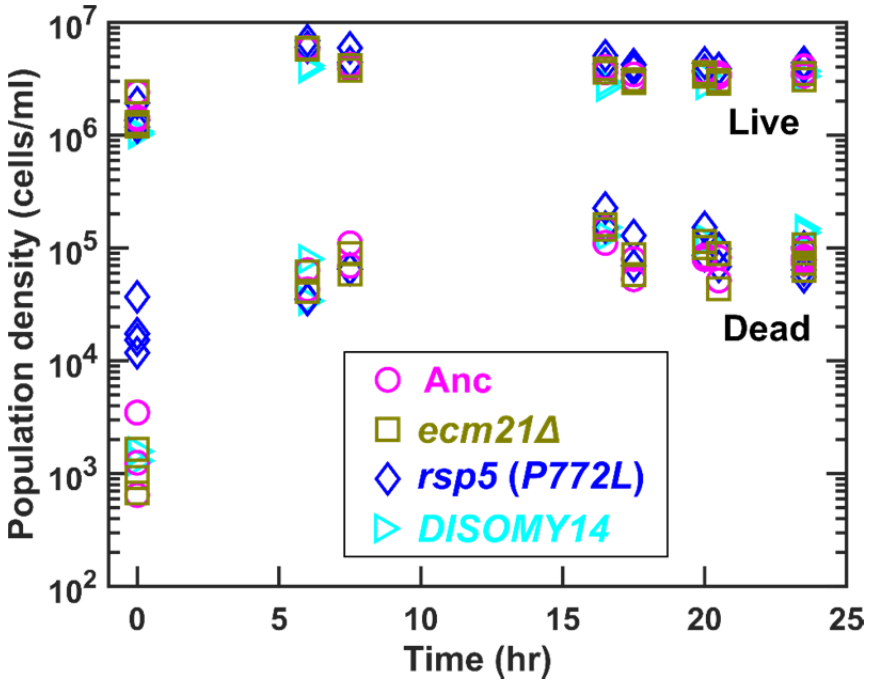

Table 1. Mutations that repeatedly arose in independent lines

Table 1 Single-nucleotide polymorphisms (SNPs) and chromosomal duplications from Illumina re-sequencing of $L^{-}H^{+}$ from CoSMO communities (top) and lysine-limited chemostats (bottom). All clones except for two (WY1592 and WY1593 of line B3 at Generation 14) had either an *ecm21* or an *rsp5* mutation, often in conjunction with chromosome 14 duplication. Note that the RM11 strain background in this study differed from the S288C strain background used in our earlier study [21]. This could explain, for example, why mutations in *DOA4* were repeatedly observed in the earlier study [21] but not here. For a schematic diagram of the locations of mutations with respect to protein functional domains in *ecm21* and *rsp5*, see Figure 2 Figure Supplement 1. For other mutations, see Table 1-Source Data 1.

L-H+	**line**	**gen**	***ecm21***	***rsp5***	**chromosome duplicated**	**strain**
CoSMO comm.	A1	24	Glu316 -> Stop	--	11, 14	WY1588
			--	Pro772 -> Leu	11	WY1589
		151	--	Pro772 -> Leu	--	WY1590
			--	Pro772 -> Leu	11, 14, 16	WY1591
	B1	25	Leu812->Stop	--	14	WY1584
		49	--	Gly689 -> Cys	14	WY1585
		76	--	Gly689 -> Cys	--	WY1586
				Gly689 -> Cys	14	WY2467
			--	Gly689 -> Cys	14	WY1587
	B3	14	--	--	--	WY1592
			--	--	14	WY1593
		34	Arg742 -> Stop	--	14, 16	WY1594
			Arg742 -> Stop	--	14, 16	WY1595
		63	Arg742 -> Stop	Arg742 -> His	12, 14	WY1596
lysine-limited chemostat mono-culture	7.Line1	30	Asp652 frameshift		14	WY1601
			Glu216 -> Stop		14	WY1602
	7.Line2	30	Pro886 -> Ser		11, 14, 16	WY1603
	7.Line3	30	Thr586 frameshift		14	WY1604
			Thr586 frameshift		14	WY1605
	11.Line1	19	Glu688 -> Stop		14, 16	WY1606

				G(-281) ->A	--	WY1608
	11.Line2	19		A(-304) -> G	--	WY1607
		50	Glu793 frameshift		14	WY1609

480

481 ***Table 1-Source Data 1. Summary of mutations***

482 ***Supplementary file 1. List of strains***

483

484 # Acknowledgement

485 We thank Aric Capel for the chemostat evolution experiment data, and Jose Pineda for an earlier
486 collaboration that eventually led to this discovery. We also thank members of the Shou lab (Li Xie, David
487 Skelding, Alex Yuan, Sonal) for discussions.

488 # References

489 1. Maynard Smith J. Evolution and the theory of games. Cambridge; New York: Cambridge University
490 Press; 1982.

491 2. Sachs JL, Mueller UG, Wilcox TP, Bull JJ. The evolution of cooperation. The Quarterly Review of
492 Biology. 2004;79(2):135–160.

493 3. Michod RE, Roze D. Cooperation and conflict in the evolution of multicellularity. Heredity. 2001
494 Jan;86(1):1–7.

495 4. Boucher DH. The Biology of Mutualism: Ecology and Evolution. Boucher DH, editor. New York:
496 Oxford University Press; 1985.

497 5. Cook JM, Rasplus JY. Mutualists with attitude: coevolving fig wasps and figs (vol 18, pg 241, 2003).
498 Trends in Ecology & Evolution. 2003 Jul;18(7):325–325.

499 6. Zientz E, Dandekar T, Gross R. Metabolic interdependence of obligate intracellular bacteria and
500 their insect hosts. Microbiology and Molecular Biology Reviews. 2004 Dec;68(4):745–770.

501 7. Gil R, Latorre A. Unity Makes Strength: A Review on Mutualistic Symbiosis in Representative Insect
502 Clades. Life (Basel). 2019 Feb 25;9(1). PMID: 30823538

503 8. Aktipis C. Athena, Boddy Amy M., Jansen Gunther, Hibner Urszula, Hochberg Michael E., Maley
504 Carlo C., Wilkinson Gerald S. Cancer across the tree of life: cooperation and cheating in

multicellularity. Philosophical Transactions of the Royal Society B: Biological Sciences. 2015 Jul 19;370(1673):20140219.

9. Gano-Cohen KA, Wendlandt CE, Stokes PJ, Blanton MA, Quides KW, Zomorrodian A, Adinata ES, Sachs JL. Interspecific conflict and the evolution of ineffective rhizobia. Ecol Lett. 2019 Mar 18; PMID: 30887662

10. Kiers ET, Rousseau RA, West SA, Denison RF. Host sanctions and the legume–rhizobium mutualism. Nature. 2003 Sep 4;425(6953):78–81.

11. Bshary R, Grutter AS. Image scoring and cooperation in a cleaner fish mutualism. Nature. 2006 Jun 22;441(7096):975–978.

12. Shou W. Acknowledging selection at sub-organismal levels resolves controversy on pro-cooperation mechanisms. eLife. 2015 Dec 29;4:e10106.

13. Chao L, Levin BR. Structured habitats and the evolution of anticompetitor toxins in bacteria. Proc Natl Acad Sci U S A. 1981 Oct;78(10):6324–8. PMCID: 349031

14. Momeni B, Waite AJ, Shou W. Spatial self-organization favors heterotypic cooperation over cheating. Elife. 2013;2:e00960. PMCID: PMC3823188

15. Harcombe W. Novel cooperation experimentally evolved between species. Evolution. 2010;64(7):2166–2172. PMID: 20100214

16. Nowak MA. Five Rules for the Evolution of Cooperation. Science. 2006 Dec 8;314(5805):1560–1563.

17. Pande S, Kaftan F, Lang S, Svatoš A, Germerodt S, Kost C. Privatization of cooperative benefits stabilizes mutualistic cross-feeding interactions in spatially structured environments. The ISME Journal. 2016 Jun;10(6):1413–1423.

18. Harcombe WR, Chacón JM, Adamowicz EM, Chubiz LM, Marx CJ. Evolution of bidirectional costly mutualism from byproduct consumption. Proceedings of the National Academy of Sciences. 2018;115(47):12000–12004.

19. Asfahl KL, Walsh J, Gilbert K, Schuster M. Non-social adaptation defers a tragedy of the commons in Pseudomonas aeruginosa quorum sensing. ISME J. 2015 Jan 23; PMID: 25615439

20. Morgan AD, Quigley BJZ, Brown SP, Buckling A. Selection on non-social traits limits the invasion of social cheats. Ecology Letters. 2012;15(8):841–846. PMID: 22639835

21. Waite AJ, Shou W. Adaptation to a new environment allows cooperators to purge cheaters stochastically. PNAS. 2012 Nov 20;109(47):19079–19086. PMID: 23091010

22. Foster KR, Shaulsky G, Strassmann JE, Queller DC, Thompson CR. Pleiotropy as a mechanism to stabilize cooperation. Nature. 2004 Oct 7;431(7009):693–6.

23. Dandekar AA, Chugani S, Greenberg EP. Bacterial quorum sensing and metabolic incentives to cooperate. Science. 2012 Oct 12;338(6104):264–266. PMID: 23066081

24. Oslizlo A, Stefanic P, Dogsa I, Mandic-Mulec I. Private link between signal and response in Bacillus subtilis quorum sensing. Proceedings of the National Academy of Sciences. 2014;111(4):1586–1591.

25. Harrison F, Buckling A. Siderophore production and biofilm formation as linked social traits. The ISME Journal. 2009 May;3(5):632–634.

26. Sathe S, Mathew A, Agnoli K, Eberl L, Kümmerli R. Genetic architecture constrains exploitation of siderophore cooperation in the bacterium Burkholderia cenocepacia. Evolution Letters. 2019;3(6):610–622.

27. dos Santos M, Ghoul M, West SA. Pleiotropy, cooperation, and the social evolution of genetic architecture. PLOS Biology. Public Library of Science; 2018 Oct 25;16(10):e2006671.

28. Frénoy A, Taddei F, Misevic D. Genetic Architecture Promotes the Evolution and Maintenance of Cooperation. PLOS Computational Biology. 2013 Nov 21;9(11):e1003339.

29. Hart SFM, Mi H, Green R, Xie L, Pineda JMB, Momeni B, Shou W. Uncovering and resolving challenges of quantitative modeling in a simplified community of interacting cells. PLOS Biology. 2019 Feb 22;17(2):e3000135.

30. Hart SFM, Pineda JMB, Chen C-C, Green R, Shou W. Disentangling strictly self-serving mutations from win-win mutations in a mutualistic microbial community. eLife. 2019 Jun 4;8:e44812.

31. Rakoff-Nahoum S, Foster KR, Comstock LE. The evolution of cooperation within the gut microbiota. Nature. 2016 Apr 25; PMID: 27111508

32. Schubert KR. Products of Biological Nitrogen Fixation in Higher Plants: Synthesis, Transport, and Metabolism. Annual Review of Plant Physiology. 1986;37(1):539–574.

33. Beliaev AS, Romine MF, Serres M, Bernstein HC, Linggi BE, Markillie LM, Isern NG, Chrisler WB, Kucek LA, Hill EA, Pinchuk GE, Bryant DA, Steven Wiley H, Fredrickson JK, Konopka A. Inference of interactions in cyanobacterial–heterotrophic co-cultures via transcriptome sequencing. ISME J. 2014 Nov;8(11):2243–2255.

34. Helliwell KE, Wheeler GL, Leptos KC, Goldstein RE, Smith AG. Insights into the Evolution of Vitamin B12 Auxotrophy from Sequenced Algal Genomes. Molecular Biology and Evolution. 2011 Oct 1;28(10):2921–2933.

35. Carini P, Campbell EO, Morré J, Sañudo-Wilhelmy SA, Cameron Thrash J, Bennett SE, Temperton B, Begley T, Giovannoni SJ. Discovery of a SAR11 growth requirement for thiamin's pyrimidine precursor and its distribution in the Sargasso Sea. ISME J. 2014 Aug;8(8):1727–1738.

36. Rodionova IA, Li X, Plymale AE, Motamedchaboki K, Konopka AE, Romine MF, Fredrickson JK, Osterman AL, Rodionov DA. Genomic distribution of B-vitamin auxotrophy and uptake transporters in environmental bacteria from the C hloroflexi phylum. Environmental microbiology reports. 2015;7(2):204–210.

37. Zengler K, Zaramela LS. The social network of microorganisms — how auxotrophies shape complex communities. Nature Reviews Microbiology. 2018 Mar 29;1.

38. Jiang X, Zerfaß C, Feng S, Eichmann R, Asally M, Schäfer P, Soyer OS. Impact of spatial organization on a novel auxotrophic interaction among soil microbes. The ISME Journal. 2018 Mar 23;1.

39. Momeni B, Brileya KA, Fields MW, Shou W. Strong inter-population cooperation leads to partner intermixing in microbial communities. elife. 2013;2:e00230. PMCID: 3552619

40. Shou W, Ram S, Vilar JM. Synthetic cooperation in engineered yeast populations. Proc Natl Acad Sci USA. 2007;104:1877–1882. PMCID: 1794266

41. Peters J, Janzing D, Schölkopf B. Elements of causal inference: foundations and learning algorithms. MIT press; 2017.

42. Green R, Sonal, Wang L, Hart SFM, Lu W, Skelding D, Burton JC, Mi H, Capel A, Chen HA, Lin A, Subramaniam AR, Rabinowitz JD, Shou W. Metabolic excretion associated with nutrient–growth dysregulation promotes the rapid evolution of an overt metabolic defect. PLOS Biology. Public Library of Science; 2020 Aug 24;18(8):e3000757.

43. Hart SFM, Skelding D, Waite AJ, Burton JC, Shou W. High-throughput quantification of microbial birth and death dynamics using fluorescence microscopy. Quant Biol [Internet]. 2019 Jan 4 [cited 2019 Feb 26]; Available from: https://doi.org/10.1007/s40484-018-0160-7

44. Lin CH, MacGurn JA, Chu T, Stefan CJ, Emr SD. Arrestin-Related Ubiquitin-Ligase Adaptors Regulate Endocytosis and Protein Turnover at the Cell Surface. Cell. 2008 Nov 14;135(4):714–725. PMID: 18976803

45. Jones CB, Ott EM, Keener JM, Curtiss M, Sandrin V, Babst M. Regulation of Membrane Protein Degradation by Starvation-Response Pathways. Traffic. 2012;13(3):468–482. PMID: 22118530

46. Hart SFM, Pineda JMB, Chen CC, Green R, Shou W. Disentangling strictly self-serving mutations from win-win mutations in a mutualistic microbial community. eLife, accepted. 2019;

47. Mitri S, Foster KR. Pleiotropy and the low cost of individual traits promote cooperation. Evolution. 2016;70(2):488–494.

48. Chisholm RH, Connelly BD, Kerr B, Tanaka MM. The Role of Pleiotropy in the Evolutionary Maintenance of Positive Niche Construction. The American Naturalist. The University of Chicago Press; 2018 Jul 1;192(1):35–48.

49. Queller DC. Pleiotropy and synergistic cooperation. PLOS Biology. Public Library of Science; 2019 Jun 21;17(6):e3000320.

50. Gurney J, Azimi S, Brown SP, Diggle SP. Combinatorial quorum sensing in Pseudomonas aeruginosa allows for novel cheating strategies. Microbiology,. Microbiology Society,; 2020;166(8):777–784.

51. Hosoda K, Suzuki S, Yamauchi Y, Shiroguchi Y, Kashiwagi A, Ono N, Mori K, Yomo T. Cooperative Adaptation to Establishment of a Synthetic Bacterial Mutualism. PLoS ONE. 2011 Feb 16;6(2):e17105.

52. Boone C, Bussey H, Andrews BJ. Exploring genetic interactions and networks with yeast. Nat Rev Genet. 2007 Jun;8(6):437–449.

53. Müller MJI, Neugeboren BI, Nelson DR, Murray AW. Genetic drift opposes mutualism during spatial population expansion. PNAS. 2014 Jan 21;111(3):1037–1042. PMID: 24395776

54. Fritts RK, Bird JT, Behringer MG, Lipzen A, Martin J, Lynch M, McKinlay JB. Enhanced nutrient uptake is sufficient to drive emergent cross-feeding between bacteria in a synthetic community. The ISME Journal. Nature Publishing Group; 2020 Nov;14(11):2816–2828.

55. Toulmay A, Schneiter R. A two-step method for the introduction of single or multiple defined point mutations into the genome of Saccharomyces cerevisiae. Yeast. 2006;23(11):825–831.

56. Armitt S, Woods RA. Purine-excreting mutants of Saccharomyces cerevisiae. I. Isolation and genetic analysis. Genet Res. 1970 Feb;15(1):7–17. PMID: 5415229

57. Feller A, Ramos F, Pierard A, Dubois E. In Saccharomyces cerevisae, feedback inhibition of homocitrate synthase isoenzymes by lysine modulates the activation of LYS gene expression by Lys14p. Eur J Biochem. 1999 Apr;261(1):163–70.

58. Skelding DH, Hart SFM, Vidyasagar T, Pozhitkov AE, Shou W. Developing a low-cost milliliter-scale chemostat array for precise control of cellular growth. Quant Biol. 2018 Jun 1;6:129–141.

59. Nikko E, Sullivan JA, Pelham HRB. Arrestin-like proteins mediate ubiquitination and endocytosis of the yeast metal transporter Smf1. EMBO reports. 2008 Dec 1;9(12):1216–1221.

60. Hein C, Springael JY, Volland C, Haguenauer-Tsapis R, André B. NPl1, an essential yeast gene involved in induced degradation of Gap1 and Fur4 permeases, encodes the Rsp5 ubiquitin-protein ligase. Mol Microbiol. 1995 Oct;18(1):77–87. PMID: 8596462